Carbohydrate Research 346 (2011) 1752–1759

Contents lists available at ScienceDirect

Carbohydrate Research

journal homepage: www.elsevier.com/locate/carres

Phenylboronic acid esters of the common 2-deoxy-aldoses

David Heß, Peter Klüfers *

Ludwig-Maximilians-Universität, Department Chemie, Butenandtstraße 5-13, 81377 München, Germany

ARTICLE INFO

Article history:
Received 4 April 2011
Received in revised form 24 May 2011
Accepted 27 May 2011
Available online 21 July 2011

Keywords:
Deoxy-glycoses
Phenylboronic acid esters
Aldehydo isomers

ABSTRACT

Phenylboronic acid esters are formed by the three common 2-deoxy aldoses: 2-deoxy-D-*erythro*-pentose ('2-deoxy-D-ribose'), 2-deoxy-D-*lyxo*-hexose ('2-deoxy-D-galactose'), and 2-deoxy-D-*arabino*-hexose ('2-deoxy-D-glucose'). The major species that was formed from equimolar quantities of boronic acid and the aldose, was the 3,4-monoester of the pentopyranose in a skew-boat conformation, and the 4,6-monoester in the case of the two hexopyranoses. A double molar quantity of boronic acid led, for both 2-deoxy-hexoses, to the diester of the open-chain aldehydo isomer as the major product: the 3,5:4,6-diester for the lyxo-configured deoxy-hexose, and the 3,4:5,6-diester of the arabino-configured isomer. Minor products of all reactions were identified by a combined NMR/DFT methodology.

1. Introduction

The coordination chemistry of the glycoses ('reducing sugars', aldoses and ketoses) is governed by the unusual adaptability of their chelating O-atom pattern to a (semi)metal's pattern of ligand-binding sites. In contrast to a usual ligand that is able to match its ligating donor sites to the metal centre by adapting only its conformation, a glycose's variability is unique because its configuration is adaptable as well. Due to the coexistence of the various isomers (pyranose, furanose, open-chain forms) in a glycose's solution equilibrium, a dynamic ligand library is thus provided to a central metal. In addition, common conformational matching is available for the more flexible isomers such as the furanose anomers. Stable chelates require a deprotonation of the coordinating hydroxy functions. Depending on the metal's Lewis acidity, the more acidic anomeric hydroxy function is either a preferred binding site (weak-to-moderate Lewis acidity), or it is avoided if a central metal's Lewis acidity is so high that it prefers bonding to the strongly basic alkoxide functions stemming from the weakly acidic alcoholic hydroxy group.

The phenylborylene moiety provides a small semimetal centre of intermediate-to-strong acidity. Accordingly, aldoses form equilibrium mixtures of phenylboronic acid esters that may include the glycose's anomeric centre but do not necessarily do so. Examples include the parent aldoses of the 2-deoxy-aldoses of this work. On the one hand, ribose forms a 2,4-chelate with its pyranose form and thus excludes the anomeric hydroxy function. On the other hand, glucose was transformed into a 1,2:3,5-diborylated furanose diester, thus including the anomeric hydroxy group.[1,2]

2-Deoxy-aldoses may be different. Due to the lack of the electron-withdrawing 2-hydroxy function, the anomeric hydroxy group is no longer significantly more acidic than the alcoholic OH functions. A metal probe that has weak-to-moderate Lewis-acidic such as palladium(II) thus loses its usual preference for chelates that include the 1-OH function and, instead, shows a mixture of chelates that is governed by rules other than the order of acidities.[3]

In this work, we will be reporting on the esters formed by phenylboronic acid and the three common 2-deoxy-aldoses derived from the 2-epimeric couples ribose/arabinose, galactose/gulose, and glucose/mannose, namely 2-deoxy-D-*erythro*-pentose (*ery*-dPen), 2-deoxy-D-*lyxo*-hexose (*lyx*-dHex), and 2-deoxy-D-*arabino*-hexose (*ara*-dHex), respectively. The analytical strategy chosen accounts for the fact that the phenylborylene residue is able to force a glycose into unstable conformations such as pyranose boats. The NMR-spectroscopic analysis, based, as in related work, on 2D techniques and the use of Karplus relationships to identify the isomer in question, thus did not reach the same degree of confidence as in the palladium-based work. The reason was that the last step of the latter can use the so-called 'coordination-induced shift' (CIS) to identify heteroatom binding in a five-membered chelate ring by a typical downfield shift of the respective ^{13}C NMR signals. A prerequisite of the CIS determination is the availability of the chemical shifts of the free, non-derivatised glycose isomer as the reference state. The method thus is not applicable if the spectra of the reference molecules are unknown due to either a too small amount of the respective glycose isomer or the glycose's transformation to an unstable conformation in the chelate. In the compounds of this work, both obstacles had to be surmounted, as well as the pronounced tendency of the boron centre to form six-membered chelate rings which give rise to a less characteristic CIS pattern.

* Corresponding author.
E-mail address: kluef@cup.uni-muenchen.de (P. Klüfers).

0008-6215/$ - see front matter © 2011 Elsevier Ltd. All rights reserved.
doi:10.1016/j.carres.2011.05.031

As a substitute for the lacking CIS-based arguments, we chose a computer-chemical approach. The Karplus-relationship-based procedure thus was either followed by or just replaced by a first-principles calculation of the molecules that appeared to be possible alternatives, and their calculated ^{13}C NMR shift pattern was compared with the experimental spectrum to identify the correct molecular structure.[2] The method was validated for 2-deoxy-glycoses by the investigation of a methyl aldopyranoside of each 2-deoxy-aldose of this work, namely Me-β-*ery*-dPen*p*, Me-α-*lyx*-dHex*p*, and Me-α-*ara*-dHex*p* (following IUPAC usage, in this work '*p*' denotes a pyranose, '*f*' a furanose). The three glycosides are well-suited for a calibration procedure since they are configurationally fixed, have restricted chelating properties because of the lack of a 1-OH function, and afforded crystal-structure analysis of their borylene derivatives.

2. Results and discussion

2.1. 2-Deoxy-pyranosides

The only product of the reaction of equimolar quantities of phenylboronic acid and methyl 2-deoxy-β-D-*erythro*-pentopyranoside (Me-β-*ery*-dPen*p*) showed some of the mentioned features. A Karplus-relationship-based analysis resulted in a skew-boat conformation of the product which went along with an almost eclipsed conformation of the former 3,4-diol function. The conformation was indicative of the esterification of the 3,4-diol function. In agreement with the formation of a five-membered chelate ring, the significant downfield shifts of the ^{13}C3 and ^{13}C4 NMR signals were expected (Table 1). However, the conformational change was also observable by the large upfield shifts of the remaining pyranose-atom signals. In a DFT approach, the ^{13}C NMR shift pattern was reproduced with a mean deviation of 1.1 ppm, and a maximum deviation of 2.4 ppm for the anomeric carbon. Crystal-structure analysis showed the conformation of the pyranose ring more precisely. In crystals of BPh(Me-β-*ery*-dPen*p*3,4H$_{-2}$) (**1b**), the chelate ring, which is annellated to the pyranose skew boat, is almost flat in terms of O3–C3–C4–O4 torsion (Fig. 1).

The investigation on the β-anomer was completed by spectroscopic/DFT work on the respective α glycoside (**1a**). The results

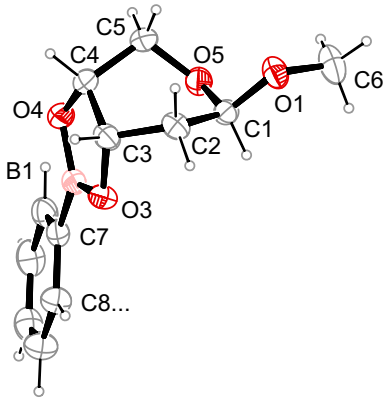

Figure 1. ORTEP representation of the molecular structure of BPh(Me-β-*ery*-dPen*p*3,4H$_{-2}$) in crystals of **1b** (40% probability ellipsoids). Distances (Å) and angles (°): B1–O3 1.366(2), B1–O4 1.368(2), O3–B1–O4 113.6(2); O1–C1–C2–C3 151.4(2), O3–C3–C4–O4: 9.2(2)°. Puckering Å parameters of the pyranose ring O5–C1–…: Q = 0.704(2) Å, θ = 95.5(2)°, φ = 141.1(2)°, which resembles a skew-boat conformation between $^{2}S_{O}$ and $^{2,5}B$. The flat chelate ring (Q = 0.089(2) Å, φ = 268(1)°) is slightly $^{4}T_{3}$-twisted.[17]

are compiled in the Section 4 (^{1}H NMR spectra) and in Table 1 (^{13}C NMR spectra).

The methyl 2-deoxy-D-hexopyranosides, both the lyxo- and the arabino-configured isomer, reacted with an equimolar amount of phenylboronic acid under 4,6-esterification. The crystal-structure analyses of BPh(Me-α-*lyxo*-dHex*p*4,6H$_{-2}$) (**2**) (Fig. 2) and BPh(Me-α-*arabino*-dHex*p*4,6H$_{-2}$) (**3**) (Fig. 3) showed molecules whose pyranose part resides in the stable $^{4}C_{1}$ chair whereas a half-chair conformation resulted for the chelate rings. The observation that six-membered chelate rings give rise to a CIS pattern different from that of their five-membered counterparts (weakly downfield–strongly upfield–weakly downfield for the three carbons of the six-membered cycle versus strongly downfield–strongly downfield for the vicinal diol's carbons of a five-membered chelate), is obvious from Table 1. At the same time, the shifts related to the carbon atoms in the vicinity to the chelate were minor in agreement with a smaller alteration of the conformation in the borylated and the reference state. The match of DFT-calculated

Table 1
Experimental (δ_{exp}) and calculated (δ_{calcd}) ^{13}C NMR chemical shifts (ppm) of the boronic-acid esters of the 2-deoxy-pyranosides **1**–**3** in DMSO-d_6

		C1	C2	C3	C4	C5	C6	OMe
1a	δ_{exp}	97.8	33.3	71.8	72.6	61.6		54.8
	δ_{calcd}	95.4	32.7	70.8	72.4	61.7		52.4
	$\delta_{exp} - \delta_{calcd}$	2.4	0.6	1.0	0.2	−0.1		2.4
	δ_{ref}	100.4	35.0	67.1	66.6	65.1		55.3
	$\delta_{exp} - \delta_{ref}$	−2.6	−1.7	4.7	6.0	−3.5		−0.5
1b	δ_{exp}	96.4	30.4	72.0	74.5	61.0		54.5
	δ_{calcd}	94.7	31.1	72.9	75.1	60.9		53.2
	$\delta_{exp} - \delta_{calcd}$	1.7	−0.7	−0.9	−0.6	0.1		1.3
	δ_{ref}	98.6	34.1	64.3	67.3	63.2		54.5
	$\delta_{exp} - \delta_{ref}$	−2.2	−3.7	7.7	7.2	−2.2		0.0
2	δ_{exp}	98.6	32.1	63.6	69.8	64.4	64.9	54.4
	δ_{calcd}	97.8	33.4	65.8	70.1	64.7	65.2	53.4
	$\delta_{exp} - \delta_{calcd}$	0.8	−1.3	−2.2	−0.3	−0.3	−0.3	−1.0
	δ_{ref}	98.0	32.7	64.8	67.4	71.3	61.1	53.9
	$\delta_{exp} - \delta_{ref}$	0.6	−0.6	−1.2	2.4	−6.9	3.8	0.5
3	δ_{exp}	98.5	38.1	66.2	77.0	64.6	63.8	54.3
	δ_{calcd}	98.0	37.7	67.1	77.2	64.0	64.3	53.4
	$\delta_{exp} - \delta_{calcd}$	0.5	0.4	−0.9	−0.2	0.6	−0.5	0.9
	δ_{ref}	97.7	37.9	68.1	71.7	73.1	61.1	53.8
	$\delta_{exp} - \delta_{ref}$	0.8	0.2	−1.9	5.3	−8.5	2.7	0.5

δ_{ref} denotes chemical shifts of the free glycosides in the same solvent. $\delta_{exp} - \delta_{ref}$ is the coordination-induced shift (CIS).

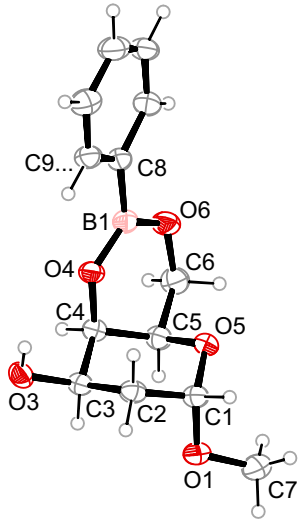

Figure 2. ORTEP representation of the molecular structure of BPh(Me-α-*lyxo*-dHex*p*4,6H$_{-2}$) in crystals of **2** (40% probability ellipsoids). Distances (Å) and angles (°): B1–O4 1.369(3), B1–O6 1.362(3), O4–B1–O6 122.9 (3). Puckering parameters: pyranose ring O5–C1–…: Q = 0.550(3), θ = 0.0(3), which resembles a $^{4}C_{1}$ conformation; chelate ring B1–O4–…: Q = 0.451(3) Å, θ = 52.3(4)°, φ = 172.1(4), rather close to a ^{C5}E envelope.

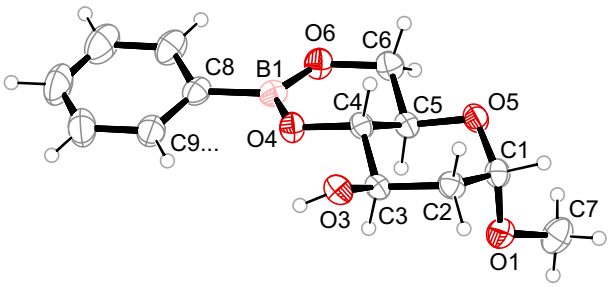

Figure 3. ORTEP representation of the molecular structure of BPh(Me-α-*arabino*-dHex*p*4,6H$_{-2}$) in crystals of **3** (40% probability ellipsoids). Distances (Å) and angles (°): B1–O4 1.363(4), B1–O6 1.372(4), O4–B1–O6 122.7(3). Puckering parameters: pyranose ring O5–C1–…: $Q = 0.567(3)$, $\theta = 9.9(3)$, $\varphi = 269(2)$, which resembles a slightly distorted $^4C_1$ conformation; chelate ring B1–O4–…: $Q = 0.465(3)$ Å, $\theta = 129.0(4)°$, $\varphi = 349.1(4)$, resembling a distorted E_{C5} envelope.

and experimental shifts was 1.0 (mean) and 2.1 (maximum) for **2**, and 0.9 (mean) and 1.1 (maximum) for **3**. In the following sections, we will interpret a corresponding match of experimental and calculated shifts as indicative of a reliable structure assignment.

2.2. 2-Deoxy-glycoses

2.2.1. 2-Deoxy-D-*erythro*-pentose

With the methodological background presented in the preceding section we attempted to analyse the esters of phenylboronic acid and 2-deoxy-D-*erythro*-pentose. A DMSO solution of the free glycose showed the four cyclic isomers, namely anomeric couples of both two pyranoses and two furanoses. Three esters were detected after the workup of equimolar batches of phenylboronic acid and the deoxyaldose. The major species **4b** closely resembled the 3,4-ester of the respective methyl pyranoside in terms of its crystal structure and its NMR properties (Scheme 1, Fig. 4, Table 2). The crystallised major species was the β-anomer. The least abundant species **4a** of the three detected was the corresponding α-isomer. In agreement with DFT calculations, its conformation was assigned to a $B_{2,5}$ boat (Scheme 1). The species of intermediate quantity **4c** was assigned to the 1,3-chelate of the $^4C_1$-α-pyranose chair in terms of the DFT calculation which was supported by the detection of an H(O4) proton in the ^{1}H NMR spectrum (Table 2). The calculation resulted in a mean difference of 0.8 ppm which reliably substantiated the assignment made. The CIS values for **4c** (Table 2) nicely illustrate the point made above. Since the free α-pyranose prefers the $^1C_4$ chair, its chemical shifts are not applicable to evaluate a true CIS.[4] Accordingly, the tabulated $\delta_{exp} - \delta_{ref}$ values contain an increment from both boron binding (the CIS) and the conformational change, and thus did not permit a straightforward interpretation. As an intermediate result it might be stated that by offering two alcoholic and one hemiacetal hydroxy function, the major species was the ester of a cis-vicinal alcoholic diol function instead of the apparently strain-free α-pyranose 1,3-chelate that includes the anomeric hydroxy function.

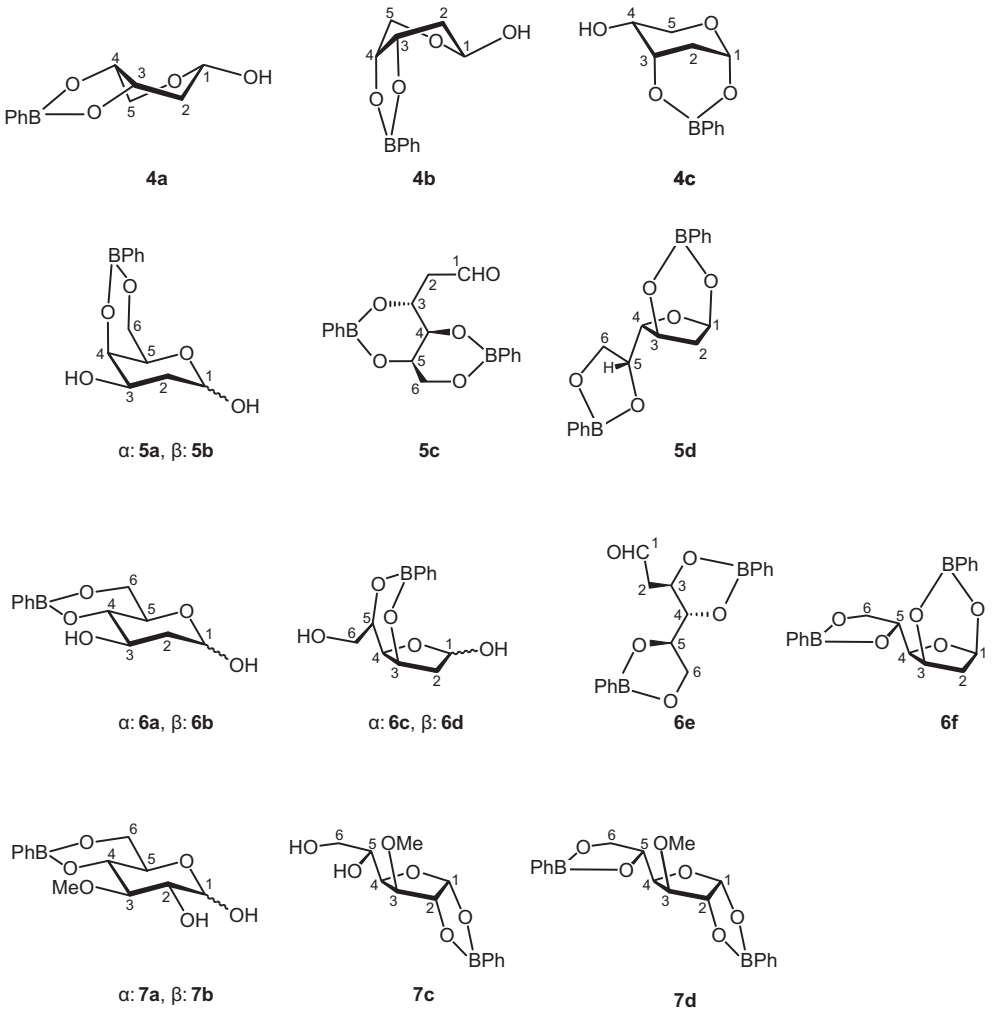

Scheme 1. Phenylboronic acid mono- and diesters.

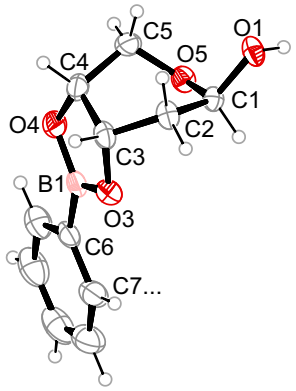

Figure 4. ORTEP representation of the molecular structure of BPh(β-*ery*-dPen*p*3,4H$_{-2}$) in crystals of **4b** (50% probability ellipsoids). Distances (Å) and angles (°): B1–O3 1.365(3), B1–O4 1.373(3), O3–B1–O4 113.7(2); torsion angles: O1–C1–C2–C3 148.4(2), O3–C3–C4–O4: 14.5(2)°. Puckering parameters of the pyranose ring O5–C1–…: Q = 0.715(2) Å, θ = 94.5(2)°, φ = 145.1(2), which resembles a $^{2}S_{O}$ skew conformation, distorted towards a $^{2,5}B$ boat. The chelate ring (Q = 0.141(2) Å, φ = 269(1)°) is $^{4}T_{3}$-twisted.[17]

Table 2
Experimental (δ_{exp}) and calculated (δ_{calcd}) ^{13}C NMR chemical shifts (ppm) of the boronic-acid esters of the 2-deoxy-glycoses **4**–**7** in DMSO-d_6

		C1	C2	C3	C4	C5	C6	OMe
4a	δ_{exp}	91.4	36.5	72.8[b]	72.4[b]	62.4		
	δ_{calcd}	89.9	35.8	72.6	72.1	60.0		
	$\delta_{exp} - \delta_{calcd}$	1.5	0.7	−0.2	0.7	2.4		
αp	δ_{ref}	93.7	36.8	67.6	66.6	65.2		
	$\delta_{exp} - \delta_{ref}$	−2.3	−0.3	5.2	5.8	−2.8		
4b	δ_{exp}	88.8	32.1	72.4	74.3	60.7		
	δ_{calcd}	88.7	31.5	73.1	75.1	60.7		
	$\delta_{exp} - \delta_{calcd}$	0.1	0.6	−0.7	−0.8	0.0		
βp	δ_{ref}	91.3	36.6	65.1	67.4	63.1		
	$\delta_{exp} - \delta_{ref}$	−2.5	−4.5	7.3	6.9	−2.4		
4c	δ_{exp}	88.4	32.3	68.4	65.9	59.5		
	δ_{calcd}	88.1	33.5	69.5	67.8	59.9		
	$\delta_{exp} - \delta_{calcd}$	0.3	−1.2	−1.1	−1.9	−0.4		
αp	δ_{ref}	93.7	36.8	67.6	66.6	65.2		
	$\delta_{exp} - \delta_{ref}$	−5.3	−4.5	0.8	−0.7	−5.7		
5a	δ_{exp}	91.4	33.3	63.5	70.2	63.9	65.2	
	δ_{calcd}	92.2	31.2	65.2	70.1	64.2	65.4	
	$\delta_{exp} - \delta_{calcd}$	−0.8	2.1	−1.7	0.1	−0.3	0.2	
αp	δ_{ref}	90.9	33.9	64.6	67.6	70.6	61.5	
	$\delta_{exp} - \delta_{ref}$	0.5	−0.6	−1.1	2.6	−6.7	4.2	
5b	δ_{exp}	93.8	36.1	67.4	69.0	67.8	65.0	
	δ_{calcd}	93.4	33.3	69.0	69.1	67.8	65.2	
	$\delta_{exp} - \delta_{calcd}$	0.4	2.8	−1.6	−0.1	0.0	−0.3	
βp	δ_{ref}	94.0	36.8	68.2	66.5	75.3	60.9	
	$\delta_{exp} - \delta_{ref}$	−0.2	−0.7	−0.8	2.5	−7.5	4.1	
5c[c,d]	δ_{exp}	197.4	47.6	69.9	68.9	64.1	65.2	
	δ_{calcd}	197.2	49.7	69.4	66.9	63.6	65.3	
	$\delta_{exp} - \delta_{calcd}$	0.2	−2.1	0.5	2.0	0.5	−0.1	
5d[d,f]	δ_{exp}	97.5	38.4	73.9	88.1	76.2	67.5	
	δ_{calcd}	96.1	37.4	72.3	90.7	77.2	67.1	
	$\delta_{exp} - \delta_{calcd}$	1.4	1.0	1.6	−2.6	−1.0	0.4	
βf	δ_{ref}	97.4	43.2	70.1	83.4	70.5	63.0	
	$\delta_{exp} - \delta_{ref}$	0.1	−4.8	3.8	4.7	5.7	4.5	
6a	δ_{exp}	91.5		65.9	77.6	64.4	64.1	
	δ_{calcd}	92.5	39.8	68.0	77.2	64.4	64.6	
	$\delta_{exp} - \delta_{calcd}$	1.0		−3.1	0.4	0.0	0.5	
αp	δ_{ref}	90.6	39.1	67.8	72.2	72.5	61.3	
	$\delta_{exp} - \delta_{ref}$	0.9		−1.9	5.4	−8.1	2.8	
6b	δ_{exp}	94.2	41.5	68.6	76.9	68.0	63.8	
	δ_{calcd}	93.4	41.5	70.5	76.3	67.5	64.3	
	$\delta_{exp} - \delta_{calcd}$	0.8	0.0	−1.9	0.6	0.5	0.5	
βp	δ_{ref}	93.5	41.4	70.9	71.7	76.9	61.4	
	$\delta_{exp} - \delta_{ref}$	0.7	0.1	−2.3	5.2	−8.9	2.4	
6c[c]	δ_{exp}	96.4	43.7	71.5	75.2	71.3	62.6	
	δ_{calcd}	96.0	43.9	73.4	76.1	72.4	64.6	
	$\delta_{exp} - \delta_{calcd}$	0.4	−0.2	−1.9	−0.9	−1.1	−2.0	
6d[c]	δ_{exp}	96.8	42.2	70.1	77.5	72.0[b]		
	δ_{calcd}	97.0	42.5	71.6	79.6	73.5	64.6	
	$\delta_{exp} - \delta_{calcd}$	0.2	0.3	1.5	2.1	1.5		
6e[c,d]	δ_{exp}	197.5	49.5	75.6	83.5	78.6	68.3	
	δ_{calcd}	197.9	52.7	77.7	83.6	79.4	69.5	
	$\delta_{exp} - \delta_{calcd}$	−0.4	−3.2	−2.1	−0.1	−0.8	−1.2	
6f[c,d]	δ_{exp}	97.1	38.7	71.4	87.7	75.0	68.9	
	δ_{calcd}	95.8	39.1	71.5	87.5	74.1	68.5	
	$\delta_{exp} - \delta_{calcd}$	1.3	−0.4	−0.1	0.2	0.9	0.4	
7a	δ_{exp}	93.2	71.6	81.5	75.6	63.8	64.1	60.2
	δ_{calcd}	93.1	74.7	80.7	73.5	63.6	64.5	59.4
	$\delta_{exp} - \delta_{calcd}$	0.1	3.1	0.8	2.1	0.2	−0.4	0.8
αp	δ_{ref}	92.3	72.0	83.5	69.8	72.1	61.1	59.9
	$\delta_{exp} - \delta_{ref}$	0.9	−0.4	−2.0	5.8	−8.3	3.0	0.3
7b	δ_{exp}	97.6	74.3	84.4	75.0	67.2	63.7	60.2
	δ_{calcd}	96.7	76.4	81.6	73.3	67.1	64.2	59.5
	$\delta_{exp} - \delta_{calcd}$	0.9	2.1	2.8	1.7	0.2	0.5	0.7
βp	δ_{ref}	96.9	74.5	86.8	69.6	76.7	61.1	59.9
	$\delta_{exp} - \delta_{ref}$	0.7	0.5	−2.4	4.7	−9.5	2.6	0.3
7c[c]	δ_{exp}	105.1	82.1	83.0	78.6	67.7	63.4	
	δ_{calcd}	104.4	81.4	82.0	79.4	69.7	66.3	55.0
	$\delta_{exp} - \delta_{calcd}$	0.8	0.7	1.0	0.8	2.0	2.9	
7d[c]	δ_{exp}	105.3	82.3	83.6	80.3	74.4	66.9	57.3
	δ_{calcd}	104.8	82.1	83.6	80.0	76.6	65.8	54.8
	$\delta_{exp} - \delta_{calcd}$	0.5	0.2	0.0	0.3	2.1	1.2	2.6
7d[c,d]	δ_{exp}	106.0	83.6	84.5	81.4	74.4	68.6	57.6
	δ_{calcd}	105.6	82.7	84.7	80.4	77.3	66.3	55.3
	$\delta_{exp} - \delta_{calcd}$	0.4	0.9	−0.2	1.0	−2.9	2.3	2.3

If available, δ_{ref} denotes chemical shifts of the respective free glycose in the same solvent. $\delta_{exp} - \delta_{ref}$ is the coordination-induced shift (CIS). For **5c**, the wrong configuration (the 3,4;5,6-diester) resulted in the $\delta_{exp} - \delta_{calcd}$ row −4.0, 0.1, −6.4, −10.2, −11.9, −2.2. For **6e**, the wrong configuration (the 3,5;4,6-diester) resulted in the $\delta_{exp} - \delta_{calcd}$ row −4.3, 2.7, 3.4, 13.0, 15.0, 3.3.

[b] May be interchanged.
[c] No CIS values due to missing assignment of the free glycose.
[d] In toluene-d_8.
[e] Is not observed in the experiment.
[f] Chemical shifts of the free glycose in DMSO-d_6.

2.2.2. 2-Deoxy-D-*lyxo*-hexose

Esters free of strain and, at the same time, without hemiacetal contribution, were found in equimolar batches of boronic acid and 2-deoxy-D-*lyxo*-hexose (*lyx*-dHex). A DMSO solution of the reaction mixture contained two products, a slightly larger quantity of BPh(α-*lyx*-dHex*p*4,6H$_{-2}$) (**5a**) and the respective β-anomer **5b**. Crystallisation succeeded from dichloromethane. Structure analysis revealed the β-anomer, **5b**, BPh(β-*lyx*-dHex*p*4,6H$_{-2}$) (Fig. 5).

Reaction of a double molar amount of phenylboronic acid with *lyx*-dHex resulted in the formation of a major (**5c**) and two minor species in terms of NMR spectroscopy in toluene solution (**5d**, **5e**). Compound **5d** was identified as the 1,3:5,6-diester of the β-furanose—supported by the lack of a H(O1) proton's ^{1}H NMR signal. No suggestion has been made as to the identity of **5e**. The major diester was completely unexpected. Compound **5c**, as the only species, exhibited a ^{13}C NMR signal typical for a free aldehyde (Table 2). The diester was formed through the four alcoholic hydroxy functions. A Karplus-relationship-based analysis favoured the 3,5:4,6-diester (two internested six-membered chelate rings) instead of the 3,4:5,6-isomer with two five-membered chelate rings

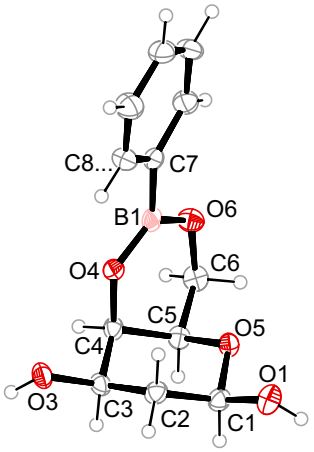

Figure 5. ORTEP representation of the molecular structure of BPh(β-*lyx*-dHex*p*4,6H$_{-2}$) in crystals of **5b** (50% probability ellipsoids). Distances (Å) and angles (°): B1–O4 1.346(6), B1–O6 1.384(6), O4–B1–O6 123.6 (4). Puckering parameters: pyranose ring O5–C1–…: $Q = 0.566(2)$ Å, $\theta = 2.6(2)°$, which resembles a $^4C_1$ conformation; chelate ring B1–O4–…: $Q = 0.480(2)$ Å, $\theta = 56.9(2)°$, $\varphi = 176.1(3)$, close to a ^{C5}E envelope.

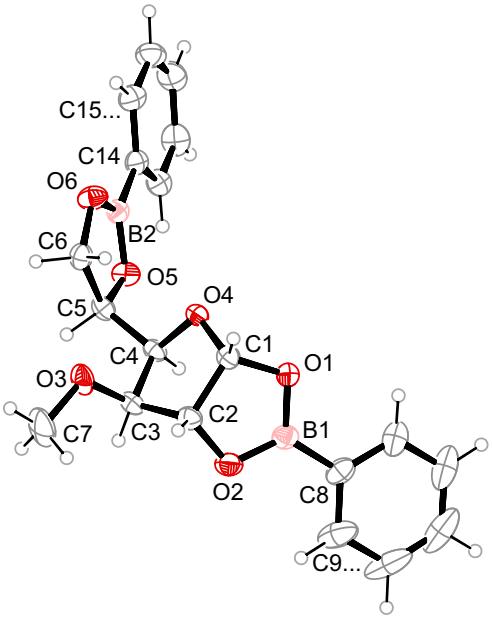

Figure 7. Structure of (**7d**). ORTEP representation of the molecular structure of (BPh)$_2$(3-*O*-Me-α-D-Glc*f*1,2;5,6H$_{-4}$) in crystals of **7d** (40% probability ellipsoids). Distances (Å) and angles (°): B1–O1 1.373(3), B1–O2 1.376(3), B2–O5 1.365(2), B2–O6 1.356(2), O1–B1–O2 112.5(2), O5–B2–O6 113.5(2); diol torsion angles: O1–C1–C2–O2 −4.6(2), O5–C5–C6–O6 −0.1(2)°. Puckering parameters of the furanose ring O4–C1–…: $Q = 0.341(2)$, $\varphi = 316.6(3)$, which resembles a conformation between $^3T_4$ and E_4. The chelate rings are almost unpuckered.

(Scheme 1). This experimental result was supported by DFT analysis. A reliable assignment was possible for the 3,5:4,6-diester only, which, moreover, revealed itself to be the stable configuration by 12 kJ mol^{-1} on the chosen level of theory. Still, it should be noted at this point that under the same experimental conditions, the glycose's nor-2-methylene derivatives D-lyxose and D-xylose do not form an open-chain aldehyde diester.

2.2.3. 2-Deoxy-D-*arabino*-hexose

The most complicated mono-esterification pattern of this work was provided by 2-deoxy-D-*arabino*-hexose (*ara*-dHex). No less than four monoesters were identified: the expected anomeric couple of the 4,6-borylene derivative of the pyranose (**6a** and **6b**), but also the 3,5-ester of the furanose anomers (**6c** and **6d**). All assignments were confirmed by DFT calculations (Table 2). In 2:1 batches of boronic acid and the glycose, the same notable result was obtained as for the lyxo-configured isomer. Besides minor quantities of an obvious β-furanose diester **6f** (Table 2) which resembles the phenylboronic acid diester of glucose, the major species **6e** exhibited an aldehyde signal in the ^{13}C NMR spectra (Fig. 6).[1] Experimental and computer-chemical assignment (Table 2) here revealed the 3,4:5,6-diester with two adjacent five-membered chelate rings instead of the motif of internested six-membered rings (Scheme 1). In agreement with this result, the non-observed 3,5:4,6-diester is 8 kJ mol^{-1} unstable with respect to the stable isomer.

The differing results for the constitution of the two open-chain diesters are rationalised by focusing on the diester moiety itself. Skipping the dangling formylmethyl functions in the two diesters transforms the 2-deoxy-D-*lyxo*-hexose derivative into the C_2-symmetrical threitol diester (BPh)$_2$(D-ThreH$_{-4}$) (Thre = threitol). The same procedure transforms the 2-deoxy-D-*arabino*-hexose diester to the C_i-symmetrical erythritol diester (BPh)$_2$(ErytH$_{-4}$) (Eryt = erythritol). Both diesters have been structurally resolved.[5] In fact, their configuration resembles the partial structures found in **5c** and **6f**. Moreover, the energy difference of the stable (the double-six-membered-ring motif) and the less stable bonding pattern is the same as found in this work. However, the preference for the centrosymmetrical double-five-ring motif is more pronounced for **6f** than for the parent structures.

2.2.4. 3-*O*-Methyl-D-glucose

As a final check on the DFT-assisted species assignment, 3-*O*-methyl-D-glucose was included in this investigation.[6] The glucose derivative has along with the deoxy-glycoses the reduction of the number of hydroxy functions by one in common. As a result of the reactions with phenylboronic acid in molar ratios of 1:1 and 2:1, the preference of alcoholic hydroxy functions as the first

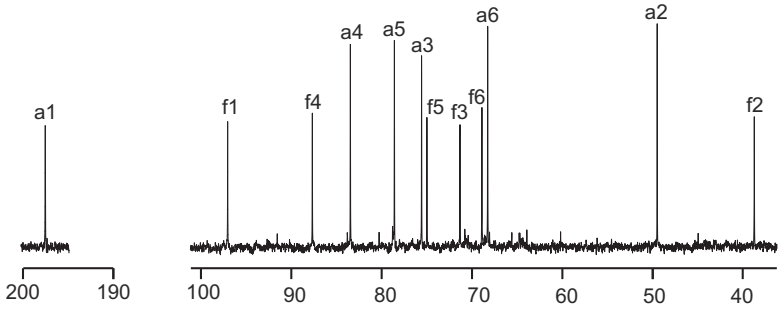

Figure 6. ^{13}C NMR spectrum of the reaction mixture of two moles of phenylboronic acid and 1 mol of 2-deoxy-D-*arabino*-hexose.

choice for esterification appears to be a loose rule of thumb. Thus, not only the expected anomeric couple of pyranose 4,6-esters (**7a** and **7b**) was observed, but also, in minor quantities, the 1,2-furanose ester **7c**. The identification of this latter compound was another example which demonstrates the benefit of the chosen methodology. CIS values are not available since no furanose isomers have been detected by means of standard NMR spectroscopy in solutions of 3-*O*-methyl-D-glucose. Hence, the required δ_{ref} values are not available. In a DFT approach, however, the mean 1.4-ppm deviation of observed and calculated shift was in the expected range for a correct assignment. With a higher boronic-acid supply, the furanose 1,2:5,6-diester **7d** was the major species. Crystallisation of the latter species succeeded. Figure 7 shows the molecular structure exhibiting the typical flat chelate rings.

3. Conclusion

Phenylboronic acid diol esters are characterised by the stereoelectronic requirements of the planar boron centre. In agreement with its sp^2 hybridisation, the O–B–O angle was expected to be about 120° (in phenylboronic acid dimethylester, without the influence of a chelate ring, the O–B–O angle was calculated as 127.7° on the same level of theory used for the diol esters). As a consequence, six-membered chelate rings adopt a half-chair conformation. Five-membered chelate rings are flat, the diol torsion angle O–C–C–O being typically in the range of 5–15°. These restrictions exclude the vicinal diol functions of a pyranose chair, both cis- and trans-configured, and lead to some strain in five-membered chelate rings. Taking 2-deoxy-D-*erythro*-pentose as an example, several esters thus seem possible: the 1,3-ester of both the α-furanose and the $^4C_1$-α-pyranose, and the 3,4-esters of the α- and the β-pyranose in a conformation close to either a $B_{2,5}$- or $^{2,5}B$-boat. Of these candidates, the 3,4-ester of the $^{2,5}B$-β-pyranose provides the major species, its $B_{2,5}$-α-anomer and the $^4C_1$-α-pyranose-1,3-ester contribute minor species. The remaining three species, the cis-1,3-furanose chelate and the 3,4-esters of both the $^{2,5}B$-α and the $B_{2,5}$-β-pyranose conformer, were unobserved. In fact, these isomers were calculated as unstable on the B3LYP/6-31+G(2d,p) level of theory (see the Supplementary data). This rule holds for the cis-1,3-furanose as long as it is needed for the formation of a second chelate.

The tendency to accept a less stable binding site to enable diester formation provided the reason for the most unexpected result of this work. Even the open-chain aldehydo isomer contributes a bis-chelator to the ligand library of the two investigated 2-deoxy-hexoses. Notably, for the two investigated 2-deoxy-hexoses, the aldehydo diester was not observed as a minor species but was the major isomer in the respective batches of 2:1 molar ratio of boronic acid and the deoxy-hexose. It should be noted that this result is obviously not transferable to the aldopentoses despite the same number of four alcoholic hydroxy functions in both glycose classes.[2]

4. Experimental section

4.1. Methods and materials

Phenylboronic acid (Aldrich), 2-deoxy-D-*erythro*-pentose ('2-deoxy-D-ribose', ABCR), 2-deoxy-D-*lyxo*-hexose ('2-deoxy-D-galactose', Glycon), 2-deoxy-D-*arabino*-hexose ('2-deoxy-D-glucose', ABCR) were used in reagent-grade quality as supplied. Methyl 2-deoxy-β-D-ribopyranoside, methyl 2-deoxy-α-D-galactopyranoside and methyl 2-deoxy-α-D-glucopyranoside were synthesised as previously described. [7–10]

NMR spectra were recorded at room temperature on a Joel Eclipse 270 (^{1}H: 270 MHz, ^{13}C: 67.9 MHz), Joel Eclipse 400 (^{1}H: 400 MHz, ^{13}C: 101 MHz) or a Joel Eclipse 500 (^{1}H: 500.16 MHz, ^{13}C: 125.77 MHz) NMR spectrometer. The signals of the deuterated solvents (^{13}C, DMSO-d_6: 39.52 ppm, toluene-d_8: 20.40 ppm) and the residual protons therein (^{1}H, DMSO-d_6: 2.50 ppm, toluene-d_8: 2.09 ppm) were used as an internal secondary reference for the chemical shift.[11] If possible, the ^{1}H and ^{13}C signals were assigned by means of DEPT135, HMQC and COSY experiments. Mass spectra were recorded on a Joel JMS-700 spectrometer in DEI$^+$ mode.

Crystals suitable for X-ray crystallography were selected by means of a polarisation microscope, mounted on a tip of a glass fibre, and subjected to XRD on either a Nonius Kappa CCD or a Stoe IPDS diffractometer, both operating with graphite-monochromated MoKα radiation (λ = 0.71073 Å). The structures were solved by direct methods (SHELXS, SIR97) and refined by full-matrix least-squares calculations on F^2 (SHELXL-97).[12,13] Hydrogen atoms were included in idealised positions, riding on their parent atoms. Anisotropic displacement parameters were refined for all non-hydrogen atoms. Crystallographic details are summarised in Table 3. All compounds, except **5b**·CH_2Cl_2, were weak anomalous scatterers. Except for **5b**·CH_2Cl_2, Friedel opposites were thus merged and the absolute structures were assigned according to the known stereochemistries of the respective starting materials.[14] A Flack parameter is thus given for **5b** only in Table 3. The refined structures were analysed with PLATON and visualised with ORTEP.[15,16] CCDC 818915 (**5b**·0.5CH_2Cl_2), 818916 (**4b**), 818917 (**7d**), 818918 (**2**), 818919 (**3**), and 818920 (**1b**) contain the supplementary crystallographic data for this paper. These data can be obtained free of charge from the Cambridge Crystallographic Data Center via www.ccdc.cam.ac.uk/data_request/cif.

Reaction of boronic acid with methyl glycopyranosides: Phenylboronic acid (1 mmol) and the respective glycopyranoside (1 mmol) were mixed with 20 mL of dioxane and refluxed in a Dean–Stark apparatus until a distillate of approximately 15 mL was collected. The remaining solvent was removed under reduced pressure. The colourless crude products were obtained in quantitative yield. Crystals were grown upon slow evaporation of solutions from dichloromethane. For NMR analysis, phenylboronic acid (1 mmol) and the respective glycopyranoside (1 mmol) were dissolved in 1 mL of DMSO-d_6 and stirred for 2 h at room temperature prior to measurement.

The reaction of boronic acid with glycoses: to a solution of the respective glycose (1 mmol) in water (1 mL) a solution of phenylboronic acid (1 or 2 mmol) in methanol (1 mL) was added. The reaction mixture was stirred for 2 h at room temperature and then evaporated to dryness under reduced pressure. The colourless crude products were obtained in quantitative yield and were analysed by mass spectrometry and NMR spectroscopy, using either DMSO-d_6 or toluene-d_8. Crystals were obtained upon slow evaporation of solutions from acetone or dichloromethane.

Details of the computational procedure applied have been documented in a previous work.[2] The structures were optimised in the gas phase at the B3LYP/6-31+G(2d,p) level of theory with very tight convergence criteria. NMR shielding constants were calculated separately for **1a–b**, **2**, **3**, **4a–c**, **5a–b**, **6a–d**, **7a–c** in DMSO and **5c–d**, **6e–f**, **7d** in toluene from the optimised structures at the PBE1PBE/6-311++G(2d,p) level of theory. The polarisable continuum model (PCM) was applied to account for solvation.

4.2. ^{1}H NMR spectra of the individual species

Compound **1a**: DMSO-d_6, 400 MHz, 20.3 °C: δ = 1.65–1.72 (m, 1H, H2a, $^2J_{2a,2b}$ 14.3 Hz), 2.27 (ddd, 1H, H2b, $^3J_{2b,3}$ 6.1 Hz), 3.24 (s, 3H, OMe), 3.83 (dd, 1H, H5a, $^2J_{5a,5b}$ 12.5 Hz), 3.89 (dd, 1H, H5b), 4.56–4.61 (sp, 2H, H1 and H4, $^3J_{1,2a}$ 7.2 Hz, $^3J_{1,2b}$ 4.1 Hz, $^3J_{4,5a}$ 4.5 Hz, $^3J_{4,5b}$ 5.4 Hz), 4.70–4.75 (m, 1H, H3).

Table 3
Crystallographic data

	1b	**2**	**3**	**4b**	**5b**·0.5CH_2Cl_2[a]	**7d**
CCDC number	818920	818918	818919	818916	818915	818917
Empirical formula	$C_{12}H_{15}BO_4$	$C_{13}H_{17}BO_5$	$C_{13}H_{17}BO_5$	$C_{11}H_{13}BO_4$	$C_{12.50}H_{16}BClO_5$	$C_{19}H_{20}B_2O_6$
M (g mol^{-1})	234.06	264.082	264.082	220.030	292.522	365.980
Colour	Colourless	Colourless	Colourless	Colourless	Colourless	Colourless
Size (mm^3)	0.13 × 0.09 × 0.06	0.24 × 0.10 × 0.07	0.31 × 0.038 × 0.024	0.39 × 0.27 × 0.21	0.29 × 0.26 × 0.22	0.44 × 0.30 × 0.08
T (K)	200(2)	200(2)	200(2)	200(2)	200(2)	173(2)
Crystal system	Orthorhombic	Monoclinic	Monoclinic	Monoclinic	Tetragonal	orthorhombic
Space group	$P2_12_12_1$	$P2_1$	$P2_1$	$P2_1$	$P4_12_12$	$P2_12_12_1$
a (Å)	5.12140(10)	10.3230(4)	11.8169(10)	6.2861(3)	11.123(2)	7.2528(6)
b (Å)	10.9441(3)	5.0832(2)	4.6576(3)	4.9563(3)	11.123	9.6512(11)
c (Å)	21.2409(5)	12.5937(6)	12.2481(10)	17.4836(11)	22.6950(6)	27.185(2)
β (°)	90	98.230(2)	95.030(4)	95.831(4)	90	90
V (Å^3)	1190.53(5)	654.03(5)	671.52(9)	541.90(5)	2807.8(6)	1902.9(3)
Z	4	2	2	2	8	4
ρ (g cm^{-3})	1.30586(5)	1.3410(1)	1.3061(2)	1.3485(1)	1.3840(3)	1.2775(2)
μ (mm^{-1})	0.095	0.101	0.098	0.100	0.285	0.092
Absorption correction	None	None	None	None	Multi-scan	Multi-scan
Reflections measured	8816	4516	4478	4203	21,610	14,220
R_{int}	0.0279	0.0348	0.0457	0.0440	0.0439	0.0354
Mean $\sigma(I)/I$	0.0201	0.0253	0.0384	0.0369	0.0441	0.0366
θ range	3.43–27.48	3.58–25.39	3.46–25.02	3.26–27.64	4.19–26.35	4.28–26.28
Reflections in refinement	1605	1333	1351	1398	2851	2217
Observed reflections	1462	1248	1131	1118	2132	1677
Parameters	155	174	174	146	179	245
Restraints	0	1	1	1	0	0
x, y (weighting scheme)	0.0521, 0.1414	0.0589, 0.1429	0.0658, 0.0084	0.0524, 0.0468	0.0500, 0	0.0341, 0
$R(F_{obs})$	0.0349	0.0405	0.0406	0.0388	0.0364	0.0289
$R_w(F^2)$	0.0942	0.1097	0.1092	0.0989	0.0875	0.0596
S	1.108	1.143	1.088	1.057	0.952	0.903
Shift/error$_{max}$	0.001	0.001	0.001	0.001	0.001	0.001
Residual densities (e Å^3)	−0.139, 0.122	−0.198, 0.180	−0.183, 0.140	−0.176, 0.151	−0.325, 0.212	−0.115, 0.128

[a] Flack parameter: −0.03(10).

Compound **1b**: DMSO-d_6, 400 MHz, 21.0 °C: δ = 1.76 (ddd, 1H, H2a, $^2J_{2a,2b}$ 15.4 Hz, $^3J_{2a,3}$ 3.3 Hz), 2.32 (ddd, 1H, H2b, $^3J_{2b,3}$ 3.6 Hz), 3.49 (s, 3H, OMe), 3.62 (d, 1H, H5a, $^2J_{5a,5b}$ 13.2 Hz), 3.80 (dd, 1H, H5b), 4.64 (dd, 1H, H4, $^3J_{4,5a}$ <1 Hz, $^3J_{4,5b}$ 1.9 Hz), 4.71 (dd, 1H, H1, $^3J_{1,2a}$ 7.7 Hz, $^3J_{1,2b}$ 5.5 Hz), 4.82 (dt, 1H, H3, $^3J_{3,4}$ 8.3 Hz).

Compound **2**: DMSO-d_6, 400 MHz, 20.3 °C: δ = 1.57–1.68 (m, 1H, H2a), 1.70–1.80 (m, 1H, H2b), 3.25 (s, 3H, OMe), 3.87–3.94 (m, 1H, H3), 4.02 (dd, 1H, H6a, $^3J_{6a,5}$ 1.1 Hz, $^2J_{6a,6b}$ 12.1 Hz), 4.23 (dd, 1H, H6b, $^3J_{6b,5}$ 1.9 Hz), 4.76–4.80 (m, 1H, H1), 4.92 (d, 1H, O3-H).

Compound **3**: DMSO-d_6, 400 MHz, 20.6 °C: δ = 1.63 (ddd, 1H, H2a, $^2J_{2a,2b}$ 13.3 Hz, $^3J_{2a,3}$ 11.3 Hz), 2.01 (dd, 1H, H2b, $^3J_{2b,3}$ 5.1 Hz), 3.26 (s, 3H, OMe), 3.62–3.68 (sp, 1H, H3), 3.68–3.73 (sp, 1H, H5, $^3J_{5,6b}$ 5.0 Hz), 3.71–3.79 (sp, 1H, H3), 3.93 (t, 1H, H6a, $^2J_{6a,6b}$ 9.9 Hz), 4.14 (dd, 1H, H6b), 4.81 (d, 1H, H1, $^3J_{1,2a}$ 3.5 Hz, $^3J_{1,2b}$ <1 Hz), 5.3 (d, 1H, O3-H).

Compound **4a**: No ^{1}H NMR signals detected.

Compound **4b**: DMSO-d_6, 400 MHz, 25 °C: δ = 1.73 (ddd, 1H, H2a, $^2J_{2a,2b}$ 15.1 Hz, $^3J_{2a,3}$ 3.3 Hz), 2.26 (ddd, 1H, H2b, $^3J_{2b,3}$ 3.9 Hz), 3.57 (d, 1H, H5a, $^2J_{5a,5b}$ 13.1 Hz), 3.90 (dd, 1H, H5b), 4.62 (dd, 1H, H4, $^3J_{4,5a}$ <1 Hz, $^3J_{4,5b}$ 1.9 Hz), 4.79–4.83 (m, 1H, H3, $^3J_{3,4}$ 8.1 Hz), 5.02–5.07 (m, 1H, H1, $^3J_{1,2a}$ 8.0 Hz, $^3J_{1,2b}$ 5.2 Hz), 6.31 (d, 1H, O1H).

Compound **4c**: DMSO-d_6, 400 MHz, 25 °C: δ = 1.99–2.11 (m, 2H, H2a+b), 3.23–3.28 (m, 1H, H5a), 3.68–3.75 (m, 1H, H5b), 3.73–3.79 (m, 1H, H4), 4.41–4.49 (m, 1H, H3), 5.2 (d, 1H, O4H), 5.42 (br, 1H, H1).

Compound **5a**: DMSO-d_6, 500 MHz, 20 °C: δ = 1.59–1.62 (m, 1H, H2a, $^2J_{2a,2b}$ 12.0 Hz), 1.71–1.75 (m, 1H, H2b), 3.96 (dd, 1H, H6a, $^2J_{6a,6b}$ 12.0 Hz), 3.98–4.04 (sp, 1H, H3), 4.17 (br, 1H, H5, $^3J_{5,6a}$ 1.1 Hz), 4.22–4.25 (m, 1H, H6b), 4.25 (sp, 1H, H4), 4.85 (d, 1H, O3-H), 5.21 (br, 1H, H1), 6.33 (dd, 1H, O1-H).

Compound **5b**: DMSO-d_6, 500 MHz, 20 °C: δ = 1.52–1.59 (m, 1H, H2a, $^2J_{2a,2b}$ 12.0 Hz), 1.74–1.77 (sp, 1H, H2b), 3.71–3.76 (m, 1H, H3), 4.02 (d, 1H, H6a, $^2J_{6a,6b}$ 11.8 Hz), 4.14–4.15 (m, 1H, H4), 4.22–4.25 (m, 1H, H6b), 4.67–4.71 (m, 1H, H1), 4.95 (d, 1H, O3-H), 6.63 (dd, 1H, O1-H).

Compound **5c**: Toluene-d_8, 400 MHz, 22 °C: δ = 1.74 (ddd, 1H, H2a, $^2J_{2a,2b}$ 16.6 Hz, $^3J_{2a,3}$ 5.6 Hz), 2.01 (ddd, 1H, H2b, $^3J_{2b,3}$ 8.6 Hz), 3.42 (t, 1H, H4, $^3J_{4,5}$ 2.2 Hz), 3.46–3.48 (m, 1H, H5, $^3J_{5,6a}$ 2.2 Hz, $^3J_{5,6b}$ 2.8 Hz), 3.57 (dd, 1H, H6a, $^2J_{6a,6b}$ 12.1 Hz), 4.03 (dd, 1H, H6b), 4.50–4.54 (m, 1H, H3, $^3J_{3,4}$ 2.2 Hz), 9.31–9.32 (m, 1H, H1, $^3J_{1,2a}$ 1.7 Hz, $^3J_{1,2b}$ 1.9 Hz).

Compound **5d**: Toluene-d_8, 400 MHz, 22 °C: δ = 1.63 (dd, 1H, H2a, $^2J_{2a,2b}$ 12.3 Hz, $^3J_{2a,3}$ <1 Hz), 2.12–2.16 (m, 1H, H2b, $^3J_{2b,3}$ 2.8 Hz), 3.69 (d, 1H, H4, $^3J_{4,5}$ 1.9 Hz), 3.73–3.79 (m, 1H, H6a), 4.00–4.04 (sp, 1H, H6b), 4.34 (d, 1H, H3, $^3J_{3,4}$ <1 Hz), 5.28 (d, 1H, H1, $^3J_{1,2a}$ <1 Hz, $^3J_{1,2b}$ 3.0 Hz).

Compound **6a**: DMSO-d_6, 400 MHz, 21 °C: δ = 1.56–1.63 (m, 1H, H2a), 1.89–1.95 (sp, 1H, H2b), 5.22–5.23 (m, 1H, H1), 6.51 (d, 1H, O1-H).

Compound **6b**: DMSO-d_6, 400 MHz, 21 °C: δ = 1.41–1.50 (m, 1H, H2a), 2.03–2.08 (m, 1H, H2b), 4.83–4.87 (m, 1H, H1), 6.87 (d, 1H, O1-H).

Compound **6c**: DMSO-d_6, 400 MHz, 21 °C: δ = 1.93–2.04 (m, 1H, H2a, $^2J_{2a,2b}$ 14.3 Hz), 2.32 (dd, 1H, H2b), 3.59–3.65 (m, 2H, H6a+b), 4.19–4.21 (m, 1H, H5), 4.27 (d, 1H, H4), 4.71 (dd, 1H, H3), 5.44–5.48 (m, 1H, H1), 6.35 (d, 1H, O1-H).

Compound **6d**: DMSO-d_6, 400 MHz, 21 °C: δ = 1.89–1.95 (sp, 1H, H2a), 2.22–2.29 (m, 1H, H2b), 5.37–5.39 (m, 1H, H1), 6.18 (d, 1H, O1-H).

Compound **6e**: Toluene-d_8, 400 MHz, 21 °C: δ = 2.05 (ddd, 1H, H2a, $^2J_{2a,2b}$ 17.1 Hz, $^3J_{2a,3}$ 5.4 Hz), 2.15 (ddd, 1H, H2b, $^3J_{2a,3}$ 7.4 Hz), 3.61–3.65 (m, 1H, H4), 3.98–4.02 (sp, 2H, H5 and H6a), 4.09–4.14 (m, 1H, H6b), 4.52–4.57 (m, 1H, H3), 9.24–9.26 (m, 1H, H1, $^3J_{1,2a}$ 1.3 Hz, $^3J_{1,2b}$ 1.7 Hz).

Compound **6f:** Toluene-d_8, 400 MHz, 21 °C: δ = 1.31 (dt, 1H, H2a, $^2J_{2a,2b}$ 12.4 Hz), 1.58 (dd, 1H, H2b, $^3J_{2b,3}$ 1.4 Hz), 3.35 (dd, 1H, H4, $^3J_{4,5}$ 8.9 Hz), 3.92–3.98 (m, 1H, H6a, $^2J_{6a,6b}$ 9.3 Hz), 4.14–

4.18 (dd, 1H, H6b), 4.35–4.37 (m, 1H, H3, $^3J_{3,4}$ 1.9 Hz), 4.44–4.50 (m, 1H, H5, $^3J_{5,6a}$ 8.0 Hz, $^3J_{5,6b}$ 6.1 Hz), 5.22 (d, 1H, H1, $^3J_{1,2a}$ 3.0 Hz, $^3J_{1,2b}$ <1 Hz).

Compound **7a**: DMSO-d_6, 400 MHz, 25 °C: δ = 3.38 Hz (sp, 1H, H2), 3.66 (s, 3H, OCH_3), 5.02 (sp, 1H, H1), 6.79 (d, 1H, O1-H).

Compound **7b**: DMSO-d_6, 400 MHz, 25 °C: δ = 3.12–3.15 (m, 1H, H2), 3.66 (s, 3H, OCH_3), 4.52–4.56 (m, 1H, H1), 5.36 (d, 1H, O2-H), 6.99 (d, 1H, O1-H).

Compound **7c**: No ^{1}H NMR signals detected.

Compound **7d**: DMSO-d_6, 400 MHz, 25 °C: δ = 3.43 (s, 3H, OCH_3), 3.98 (d, 1H, H3, $^3J_{3,4}$ 3.4 Hz), 4.27–4.31 (m, 2H, H6, $^2J_{6a,6b}$ 9.2 Hz), 4.33 (dd, 1H, H4, $^3J_{4,5}$ 6.8 Hz), 4.88 (ddd, 1H, H5, $^3J_{5,6a}$ 8.0 Hz, $^3J_{5,6a}$ 4.3 Hz), 5.03 (d, 1H, H2, $^3J_{2,3}$ <1 Hz), 6.28 (d, 1H, H1, $^3J_{1,2}$ 4.3 Hz).

Toluene-d_8, 400 MHz, 25 °C: δ = 3.06 (s, 3H, OCH_3), 3.61 (d, 1H, H3, $^3J_{3,4}$ 3.3 Hz), 4.00 (dd, 1H, H4, $^3J_{4,5}$ 6.5 Hz), 4.13 (dd, 1H, H6a, $^2J_{6a,6b}$ 9.3 Hz), 4.26 (dd, 1H, H6b), 4.30 (d, 1H, H2, $^3J_{2,3}$ <1 Hz), 4.57–4.63 (m, 1H, H5, $^3J_{5,6a}$ 8.3 Hz, $^3J_{5,6b}$ 7.2 Hz), 5.82 (d, 1H, H1, $^3J_{1,2}$ 4.4 Hz).

4.3. High-resolution DEI mass spectra

Compound **1a**: calcd for $C_{12}H_{15}BO_4$ $[M]^+$: 234.1063, found: 234.1058. Compound **1b**: calcd for $C_{12}H_{15}BO_4$ $[M]^+$: 234.1063, found: 234.1068. Compound **2**: calcd for $C_{13}H_{17}BO_5$ $[M]^+$: 264.1169, found: 264.1190. Compound **3**: calcd for $C_{13}H_{17}BO_5$ $[M]^+$: 264.1169, found: 264.1175. Compound **4**: calcd for $C_{11}H_{13}BO_4$ $[M]^+$: 220.0907, found: 220.0917. Compounds **5a**–**b**: calcd for $C_{12}H_{15}BO_5$ $[M]^+$: 250.1013, found: 250.1017. Compounds **5c**–**d**: calcd for $C_{18}H_{18}B_2O_5$ $[M]^+$: 336.1340, found: 336.1372. Compounds **6a**–**d**: calcd for $C_{12}H_{15}BO_5$ $[M]^+$: 250.1013, found: 250.0995. Compounds **6e**–**f**: calcd for $C_{18}H_{18}B_2O_5$ $[M]^+$: 336.1340, found: 336.1365. Compounds **7a**–**c**: calcd for $C_{13}H_{17}BO_6$ $[M]^+$: 280.1118, exp.: $[M]^+$ peak not found. Compound **7d**: calcd for $C_{19}H_{20}B_2O_6$ $[M]^+$: 366.1446, found: 366.1454.

Acknowledgements

We are indebted to Patrick Nimax, B.Sc., and Jessica Steinbacher, B.Sc., for their contribution in their practical courses.

Supplementary data

Supplementary data associated with this article can be found, in the online version, at doi:10.1016/j.carres.2011.05.031.

References

1. Draffin, S. P.; Duggan, P. J.; Fallon, G. D.; Tyndall, E. M. *Acta Crystallogr., Sect. E: Struct. Rep. Online* **2005**, *E61*, o1733–o1735.
2. Reichvilser, M. M.; Heinzl, C.; Klüfers, P. *Carbohydr. Res.* **2010**, *345*, 498–502.
3. Schwarz, T.; Heß, D.; Klüfers, P. *Dalton Trans.* **2010**, *39*, 5544–5555.
4. Lemieux, R. U.; Anderson, L.; Conner, A. H. *Carbohydr. Res.* **1971**, *20*, 59–72.
5. Klüfers, P.; Labisch, O. *Z. Anorg. Allg. Chem.* **2003**, *629*, 1441–1445.
6. Norrild, J. C.; Eggert, H. *J. Am. Chem. Soc.* **1995**, *117*, 1479–1484.
7. Crotti, P.; Di Bussolo, V.; Favero, L.; Macchia, F.; Pineschi, M. *Tetrahedron: Asymmetry* **1996**, *7*, 779–786.
8. Deriaz, R. E.; Overend, W. G.; Stacey, M.; Wiggins, L. F. *J. Chem. Soc.* **1949**, 2836–2841.
9. Hughes, I. W.; Overend, W. G.; Stacey, M. *J. Chem. Soc.* **1949**, 2846–2849.
10. Overend, W. G.; Shafizadeh, F.; Stacey, M. *J. Chem. Soc.* **1950**, 671–677.
11. Gottlieb, H. E.; Kotlyar, V.; Nudelman, A. *J. Org. Chem.* **1997**, *62*, 7512–7515.
12. Sheldrick, G. *Acta Crystallogr., Sect. A* **2008**, *64*, 112–122.
13. Altomare, A.; Burla, M. C.; Camalli, M.; Cascarano, G. L.; Giacovazzo, C.; Guagliardi, A.; Moliterni, A. G. G.; Polidori, G.; Spagna, R. *J. Appl. Crystallogr.* **1999**, *32*, 115–119.
14. Flack, H. D.; Bernardinelli, G. *J. Appl. Crystallogr.* **2000**, *33*, 1143–1148.
15. Spek, A. *J. Appl. Crystallogr.* **2003**, *36*, 7–13.
16. Farrugia, L. *J. Appl. Crystallogr.* **1997**, *30*, 565.
17. IUPAC *Pure Appl. Chem.* **1981**, *53*, 1901–1905.